Proteasome Inhibitors: A Novel Class of Potent and Effective Antitumor Agents

Julian Adams, Vito J. Palombella, Edward A. Sausville, et al.

Cancer Res 1999;59:2615-2622.

[CANCER RESEARCH 59, 2615–2622, June 1, 1999]

Proteasome Inhibitors: A Novel Class of Potent and Effective Antitumor Agents

Julian Adams,[1] Vito J. Palombella, Edward A. Sausville, Jill Johnson, Antonia Destree, Douglas D. Lazarus, Jochen Maas, Christine S. Pien, Samuel Prakash, and Peter J. Elliott

ProScript, Inc., Cambridge, Massachusetts 02139 [J. A., V. J. P., A. D., D. D. L., C. S. P., P. J. E.]; Hoechst Marion Roussel, D-60486 Frankfurt am Main, Germany [J. M.]; Hoechst Marion Roussel, Bridgewater, New Jersey 08807 [S. P.]; and Developmental Therapeutics Program, Division of Cancer Treatment and Diagnosis, National Cancer Institute, NIH, Bethesda, Maryland 20892 [E. A. S., J. J.]

ABSTRACT

The ubiquitin-proteasome pathway plays a critical role in the regulated degradation of proteins involved in cell cycle control and tumor growth. Dysregulating the degradation of such proteins should have profound effects on tumor growth and cause cells to undergo apoptosis. To test this hypothesis, we developed a novel series of proteasome inhibitors, exemplified by PS-341, which we describe here. As determined by the National Cancer Institute *in vitro* screen, PS-341 has substantial cytotoxicity against a broad range of human tumor cells, including prostate cancer cell lines. The PC-3 prostate cell line was, therefore, chosen to further examine the antitumor activity of PS-341. *In vitro*, PS-341 elicits proteasome inhibition, leading to an increase in the intracellular levels of specific proteins, including the cyclin-dependent kinase inhibitor, p21. Moreover, exposure of such cells to PS-341 caused them to accumulate in the G_2-M phase of the cell cycle and subsequently undergo apoptosis, as indicated by nuclear condensation and poly(ADP-ribose) polymerase cleavage. Following weekly i.v. treatment of PS-341 to mice bearing the PC-3 tumor, a significant decrease (60%) in tumor burden was observed *in vivo*. Direct injection of PS-341 into the tumor also caused a substantial (70%) decrease in tumor volume with 40% of the drug-treated mice having no detectable tumors at the end of the study. Studies also revealed that i.v. administration of PS-341 resulted in a rapid and widespread distribution of PS-341, with highest levels identified in the liver and gastrointestinal tract and lowest levels in the skin and muscle. Modest levels were found in the prostate, whereas there was no apparent penetration of the central nervous system. An assay to follow the biological activity of the PS-341 was established and used to determine temporal drug activity as well as its ability to penetrate tissues. As such, PS-341 was shown to penetrate PC-3 tumors and inhibit intracellular proteasome activity 1.0 h after i.v. dosing. These data illustrate that PS-341 not only reaches its biological target but has a direct effect on its biochemical target, the proteasome. Importantly, the data show that inhibition of this target site by PS-341 results in reduced tumor growth in murine tumor models. Together, the results highlight that the proteasome is a novel biochemical target and that inhibitors such as PS-341 represent a unique class of antitumor agents. PS-341 is currently under clinical evaluation for advanced cancers.

INTRODUCTION

The ubiquitin-proteasome pathway is the principle pathway for intracellular protein degradation (1–3). Protein substrates are "marked" with a poly-ubiquitin chain (4) and then degraded to peptides and free ubiquitin by a large multimeric protease, the proteasome, which exists within all eukaryotic cells (1–3). Numerous examples of regulatory proteins have been found to undergo ubiquitin-dependent proteolysis. Many of these proteins function as important regulators of physiological as well as pathophysiological cellular processes. Importantly, the ubiquitin-proteasome pathway plays a significant role in neoplastic growth and metastasis. The ordered and temporal degradation of numerous key proteins (*e.g.*, cyclins, CDK[2] inhibitors, and tumor suppressors) is required for cell cycle progression and mitosis (3).

The proteasome is also required for activation of NF-κB by degradation of its inhibitory protein, IκB (5). NF-κB is required, in part, to maintain cell viability through the transcription of inhibitors of apoptosis, in response to environmental stress or cytotoxic agents (6–9). Stabilization of the IκB protein and blockade of NF-κB activity has been demonstrated to make cells more susceptible to apoptosis (6–8). Furthermore, NF-κB has also been implicated in controlling the cell surface expression of adhesion molecules such as E-selectin, vascular cell adhesion molecule-1, and intercellular adhesion molecule-1 (10, 11). These cell adhesion molecules are involved in tumor metastasis and angiogenesis *in vivo* (12). During metastasis, these molecules direct the adhesion and extravasation of tumor cells to and from the vasculature to distant tissue sites.

Aberrant regulation of cell cycle proteins can result in accelerated and uncontrolled cell division, leading to tumorigenesis, cancer growth, and spread (12). Hence, proteasome inhibitors should arrest or retard cancer progression by interfering with the ordered, temporal degradation of these regulatory molecules. Inhibition of proteasome-mediated IκB degradation may limit metastasis via the attenuation of NF-κB-dependent cell adhesion molecule expression (10, 11) and make dividing cancer cells more sensitive to apoptosis (6–8). Thus, proteasome inhibitors could act through multiple mechanisms to arrest tumor growth, tumor spread, and angiogenesis, offering a novel approach to treating cancer. As such, it is understood that dosing regimens must be optimized to limit the effects of proteasome inhibition in noncancerous cells, thereby establishing a therapeutic index.

Here, we describe the development of a unique series of proteasome inhibitors that are potent, selective, and reversible. These compounds are dipeptide boronic acid analogues that inhibit the chymotryptic activity of the proteasome and, thereby, block activity of the enzyme. By attenuating the degradation of cell cycle regulatory proteins, such agents elicit multiple effects leading to the inhibition of tumor cell growth and to apoptosis. Importantly, the inhibitor potency (K_i) data correlate with the cytotoxicity profile against a panel of 60 human tumor cell lines *in vitro* as well as with *in vivo* antitumor activity in human xenograft models, supporting the mechanism of proteasome inhibition. Together, these results suggest that the mechanism of antineoplastic activity of the boronate class of compounds is unique and that proteasome inhibition represents a novel approach to the development of anticancer agents. The activity of PS-341, a representative of such compounds, was chosen to highlight the features of this novel drug class and is currently under Phase I clinical evaluation in advanced cancer patients.

MATERIALS AND METHODS

Chemical Synthesis of Inhibitors and K_i Measurements. Inhibitors were synthesized and purified according to the procedures described in Adams *et al.*

Received 12/16/98; accepted 4/2/99.

The costs of publication of this article were defrayed in part by the payment of page charges. This article must therefore be hereby marked *advertisement* in accordance with 18 U.S.C. Section 1734 solely to indicate this fact.

[1] To whom requests for reprints should be addressed, at ProScript, Inc., 38 Sidney Street, Cambridge, MA 02139. Phone: (617) 374-1470; Fax: (617) 374-1477; E-mail: jadams@proscript.com.

[2] The abbreviations used are: CDK, cyclin-dependent kinase; NF-κB, nuclear transcription factor-κB; NCI, National Cancer Institute; PARP, poly(ADP-ribose) polymerase; FACS, fluorescence-assisted cell sorting.

(13). The inhibition constant (K_i) for each inhibitor was measured according to the method of Stein *et al.* (14) using a fluorometric assay, monitoring peptide substrate cleavage of *Z*-Leu-Leu-Val-Tyr-amino methyl coumarin (*Z* = carbobenzyloxy) by the 20S proteasome.

Cell Cytotoxicity Assays. The 60-cell line panel from the NCI has been described previously (15). Each cell line was exposed to the test proteasome inhibitor in five 10-fold dilutions for a period of 48 h. The growth and viability of the treated cells was compared with that of control cells by means of sulforhodamine B anionic dye staining. The results are reported as a series of bar graphs which depict the sensitivities of each cell line to the test agent at three levels of effect: 50% growth inhibition (GI_{50}), total growth inhibition, and 50% cell kill (LC_{50}). The mean drug concentration over all 60 cell lines was calculated for each of the parameters, and the variation from the mean for each cell line was plotted. The resulting "mean graphs" reflect the pattern of cell line sensitivity for each test agent and are often characteristic of the compound's mechanism of cytotoxicity. Compounds of like mechanisms tend to have similar patterns of cell line sensitivity. The COMPARE algorithm was used to assign uniqueness of the test agent (16). Activity of the boronate proteasome inhibitors was observed across a broad range of tumor types (non-small cell lung, colon, central nervous system, melanoma, ovarian, renal, prostate and breast), including the prostate PC-3 cell line.

In additional experiments, human PC-3 prostate tumor cells were treated with PS-341 (in DMSO) for 24–48 h in complete medium. The final concentration of DMSO was 0.1%. Cytotoxicity was measured using a 3-[4,5-dimethylthiazol-2-yl]-2,5-diphenyltetrazolium bromide assay (17).

Western Blot Analysis. PC-3 cells were treated with different doses of PS-341 (in DMSO) for different periods of time as indicated on the figures. The final concentration of DMSO in the medium was 0.1%. Whole-cell extracts were prepared and analyzed by Western blots for the presence of p21, CDK-4 (Santa Cruz Biotechnology, Santa Cruz, CA), and PARP (Biomol). The secondary antibodies (1:10,000) were horseradish peroxidase-donkey antirabbit (Amersham). The blots were developed with the ECL reagent (Amersham) according to the manufacturer's instructions.

FACS Analysis. PC-3 cells were plated in six-well plates (10^6 cells/well) and grown to confluence. The cells were treated with PS-341 (100 nM) for 8 h, washed, and harvested in PBS. The cells were fixed with 70% ethanol to give a final cell concentration of 3×10^6 cells/ml. The cells were then stained with propidium iodide and the cellular DNA content was analyzed by FACS analysis according to Noguchi (18).

Nuclear Staining. PC-3 cells were treated with different doses of PS-341 for different periods of time. The cells were washed with PBS, harvested, and fixed in suspension with 3.7% formaldehyde in neutral buffer for 10 min at room temperature. The cells were centrifuged, and the cell pellet was resuspended in 0.5 ml of 80% ethanol. The cell suspension (25–50 μl) was then placed onto a microscope slide precoated with poly-L-lysine and air-dried. The slides were washed four times with 0.1% Triton X-100 in PBS. The slide was incubated with the DNA stain Hoechst 33342 (Molecular Probes; 1.0 μg/ml in PBS with 0.1% Triton-X-100) for 1.0 min. The slides were rinsed in PBS and mounted with 70% glycerol containing 25 mg/ml 1,4-diazabicyclo[2.2.2]octane. Nuclear staining was visualized using a fluorescent microscope.

Scintillation Counting. Radiolabeled [^{14}C]PS-341 (10 μCi/kg) was administered as an i.v. bolus to male mice bearing PC-3 tumors. Animals were sacrificed 1.0 h after treatment, whereupon blood and tissue samples were removed and levels of radioactivity determined using scintillation counting (Beckman).

Quantitative Whole-Body Autoradiography. Radiolabeled [^{14}C]PS-341 (0.056 MBq per animal) was administered as an i.v. bolus to male rats, which were subsequently sacrificed at 10 min, 1.0 h, 3 h, 6 h, and 24 h. Blood samples were taken at sacrifice, and levels of radioactivity were determined using combustion (Canberra-Packard system). Euthanized animals were then frozen, and sections were taken 96 h later through specific planes to identify organs of interest. Radioactivity levels in tissue were calculated using TINA software (Raytest, Straubenhard, Germany).

20S Proteasome Sample Preparation. Heparinized blood was diluted 1:1 (v/v) with saline, layered over ~1.0 ml of Nycoprep separation medium, and centrifuged at 500 × *g* for 30 min at room temperature. The WBC band was removed and washed with 3 ml of cold PBS and then centrifuged at 400 × *g* for 5 min at 4°C. The resulting pellet was resuspended in ~1.0 ml of cold PBS and microcentrifuged at 6600 × *g* for 10 min at 4°C. The cell pellet was then frozen at −80°C prior to 20S proteasome analysis. WBCs prepared above were lysed with EDTA (5 mM; pH 8.0) for 1.0 h and then centrifuged at 6600 × *g* for 10 min at 4°C. Tumor samples were lysed as above and prepared in buffer (1.0 M DTT and 1.0 M HEPES) at 1.0 g/ml and centrifuged at 2200 × *g* for 15 min at 4°C. The resultant supernatants from both sample types were then used in the assay.

Fluorometric 20S Proteasome Assay. Cell or tissue sample homogenate (5 μl) was added to 2 ml of substrate buffer (20 mM HEPES, 0.5 mM EDTA, 0.035% SDS, and 60 μM Ys substrate; pH 8.0, 37°C), and the rate of substrate cleavage/20S proteasome activity was determined. Succinyl-Leu-Leu-Val-Tyr-Amido-4-methyl-coumarin (Ys substrate) was obtained from Bachem. Other reagents were obtained from Sigma Chemical Co. (St. Louis, MO). The protein content of the samples was determined using a Coomassie protein assay (Pierce, Rockford, IL).

Animals. Male nude mice (18–20 g; $n = 51$), were obtained from the NCI (Bethesda, MD). Animals were observed for at least 1 week and examined for general health before study initiation. Animals used in these studies were asymptomatic and were housed five per cage in the animal facility at ProScript. Pellets of standard rodent chow (formula 5001; Purina, St. Louis, MO) were available *ad libitum* throughout the observation and study periods. Cambridge city tap water was provided by water bottles *ad libitum*. Male Sprague Dawley rats (200–210 g) were purchased from Charles River (Germany) and housed in the animal facility at Hoechst (Frankfurt am Main, Germany). Rats were fed milled diet (Ssniff Spezialdiaten GmbH, Soest, Germany) and allowed free access to tap water *ad libitum*. Fluorescent lighting was controlled automatically in both facilities to provide alternate light and dark cycles of ~12 h each. Temperature and humidity were centrally controlled and recorded daily.

Xenograft Procedures. PS-341 drug substance was synthesized at ProScript, Inc. (Cambridge, MA). Dose formulations of PS-341 were prepared daily during the course of the *in vivo* studies and were administered in vehicle i.v. using a dose volume of 100 μl per mouse or directly into the tumor in a 10 μl volume. Control groups were administered with the vehicle [98% saline (0.9%), 2% ethanol, and 0.1% ascorbic acid]. Due to the comparatively high levels of PS-341 in the prostate, after i.v. dosing of radiolabeled drug, it was decided to examine the effects of this novel compound in the prostate, PC-3,

Table 1 *Structure-activity relationships of 13 boronic acid proteasome inhibitors against purified proteasome activity (K_i) and their ability to inhibit cell growth across 60 tumor cell lines (average GI_{50}) from the National Cancer Institute*

Compound (NSC no./PS no.)	Structure	K_i (nM)	Average GI_{50} (nM)
681226/PS-273	MorphCONH(CHNaphthyl)CONH(CHisobutyl)B(OH)$_2$	0.2	6.3
681227/PS-293	Enantio-PS-273	2,300	56,000
681228/PS-296	8-Quinolyl sulfonylCONH(CHNaphthyl)CONH(CHisobutyl)B(OH)$_2$	3.5	17
681229/PS-303	NH$_2$(CHNaphthyl)CONH(CHisobutyl)B(OH)$_2$	12	68
681231/PS-305	MorphCONH(*s*CHNaphthyl)CONH(CHisobutyl)B(OH)$_2$	189	4,700
681234/PS-313	NaphthylCH$_2$CH$_2$CONH(CHisobutyl)B(OH)$_2$	58	1,300
681236/PS-321	MorphCONH(CHNaphthyl)CONH(CHPhe)B(OH)$_2$	0.5	6.6
681237/PS-334	CH$_3$NH(CHNaphthyl)CONH(CHisobutyl)B(OH)$_2$	3.5	13
681239/PS-341	PyrazylCONH(CHPhe)CONH(CHisobutyl)B(OH)$_2$	0.6	3.9
681242/PS-364	PheCH$_2$CH$_2$CONH(CHisobutyl)B(OH)$_2$	1,500	10,000
683086/PS-325	2-QuinolylCONH(CH*homo*Phe)CONH(CHisobutyl)B(OH)$_2$	2	34
683094/PS-352	PheCH$_2$CH$_2$CONH(CHPhe)CONH(CHisobutyl)B(OH)$_2$	0.1	10
683098/PS-383	PyridylCONH(CH*p*FPhe)CONH(CHisobutyl)B(OH)$_2$	0.6	10

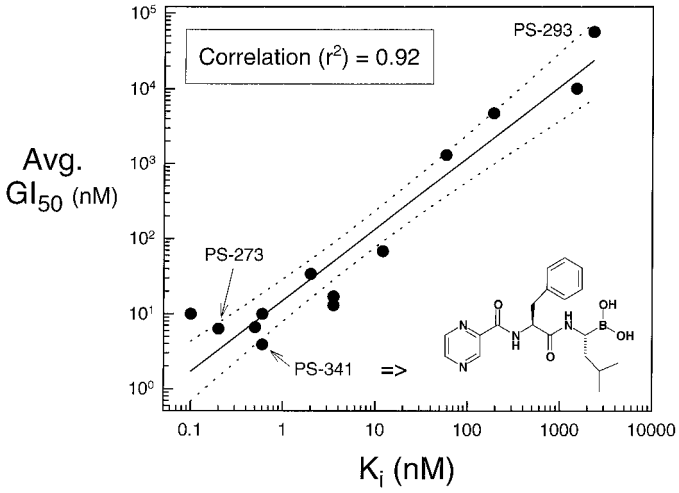

Fig. 1. Correlation (r^2) between 20S proteasome inhibitory potency (K_i) of 13 diverse dipeptide boronic acid inhibitors (●) and their ability to inhibit cell growth across 60 tumor cell lines [average GI_{50} (*Avg. GI_{50}*)] from the NCI. PS-341 was chosen for in-depth study and its structure is shown in the inset. *Data points*, log concentrations (in nM).

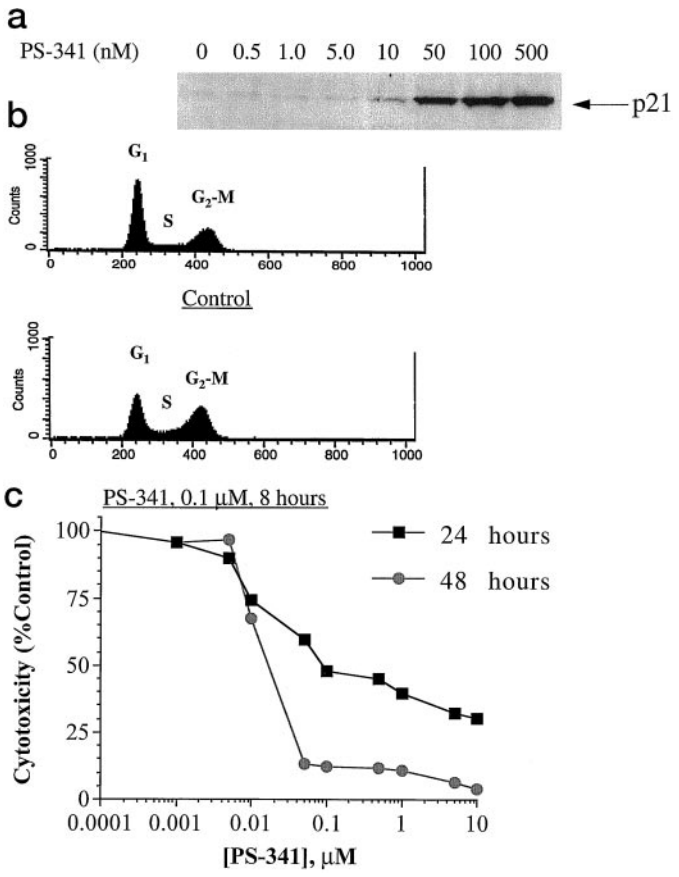

Fig. 2. PS-341 induces cell cycle arrest in PC-3 cells. *a*, increases in intracellular levels of p21 protein in PC-3 cells treated with different concentrations of PS-341 for 24 h. Whole-cell extracts were prepared and analyzed by Western blot. *b*, blockade of cell cycle progression in PC-3 cells treated with PS-341 (100 nM) for 8 h. Cells were examined using FACS analysis to determine cell cycle status. *Control*: G_1, 53.6% of cells; S, 14.5% of cells; G_2-M, 32.9% of cells. *PS-341, 0.1 μM, 8 h*: G_1, 37.6% of cells; S, 21.2% of cells; G_2-M, 42.9% of cells. *c*, cytotoxicity profile of PS-341 in PC-3 cells after 24- and 48-h exposure.

xenograft tumor model. Animals were treated when the tumors became palpable (>300 mm^3). Studies were performed according to Institutional Animal Care and Use Committee-approved procedures. Tumor volumes were calculated from the equation below using caliper measurements taken twice a week:

$$\frac{\text{Length (mm)} \times \text{width (mm)} \times \text{shortest measurement (mm)}}{2} = \text{Tumor volume } (mm^3)$$

Statistical Analysis. Tumor volume data were analyzed using ANOVA and a post hoc Dunnett's *t* test, for which $P < 0.05$ was deemed significant using a two-tailed test.

RESULTS

Synthesis of Proteasome Inhibitors. One of the first proteasome inhibitors synthesized was MG-132, a peptide aldehyde based on calpain inhibitor I (19). However, MG-132 was found to be nonselective because it inhibits other enzymes (20). The realization that the proteasome was a threonine protease (21) supported the concept that boronic acids would be potent and selective inhibitors of the proteasome (14). Such compounds form covalent and reversible complexes with the proteasome and are much more potent than their corresponding aldehydes (13). A series of selective inhibitors were prepared with K_is spanning 5 logs of potency (Table 1). The stereospecificity for drug binding is clearly demonstrated by the activity of PS-273 and the lack of potency by its inactive enantiomer PS-293 (Fig. 1). One low molecular weight, water-soluble dipeptide boronic acid, PS-341, with a K_i of 0.6 nM, was selected for intensive study (Fig. 1, *inset*).

PS-341 Is Cytotoxic for PC-3 Cells *in Vitro*. The NCI uses, as its primary preclinical assay, an *in vitro* cytotoxicity screen comprised of 60 cell lines derived from multiple human tumors (15). The average growth inhibition of 50% (GI_{50}) value for PS-341 across the entire NCI cell panel was 7 nM. Moreover, when 13 dipeptide proteasome inhibitors from the boronate series were examined, a strong correlation (Pearson coefficient, $r^2 = 0.92$) was noted after plotting K_i *versus* GI_{50} values (Fig. 1). This finding associates the intrinsic potency of this class of compounds with their antiproliferative activity in cell culture assays, confirming their activity through a biological target, the proteasome. Using the NCI's algorithm COMPARE (16), we compared the "fingerprint" for PS-341-induced cytotoxicity to the historical file of 60,000 compounds and found it to be unique, with little correlation to other "standard" or investigational agents. In addition, PS-341 was shown to penetrate into cells and inhibit proteasome-mediated intracellular proteolysis of long-lived proteins with

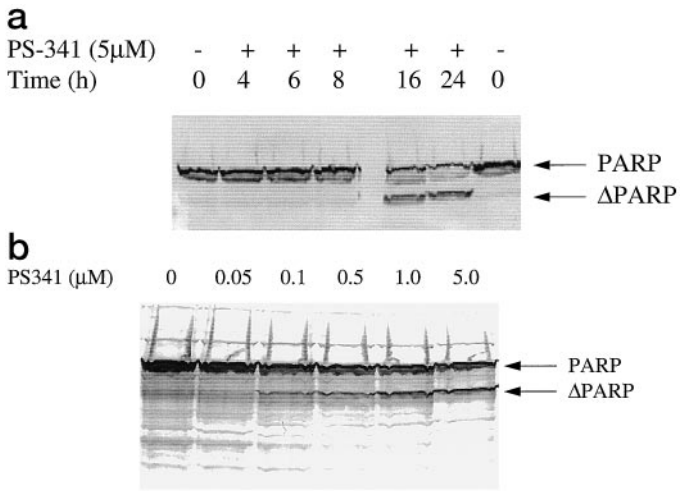

Fig. 3. PS-341 induces apoptosis in PC-3 cells. *a*, stimulation of PARP cleavage in PC-3 cells treated with PS-341 for up to 24 h. Western analysis was performed using anti-PARP antibodies. *b*, stimulation of PARP cleavage in PC-3 cells treated with different concentrations of PS-341 for 24 h. Western analysis was performed using anti-PARP antibodies.

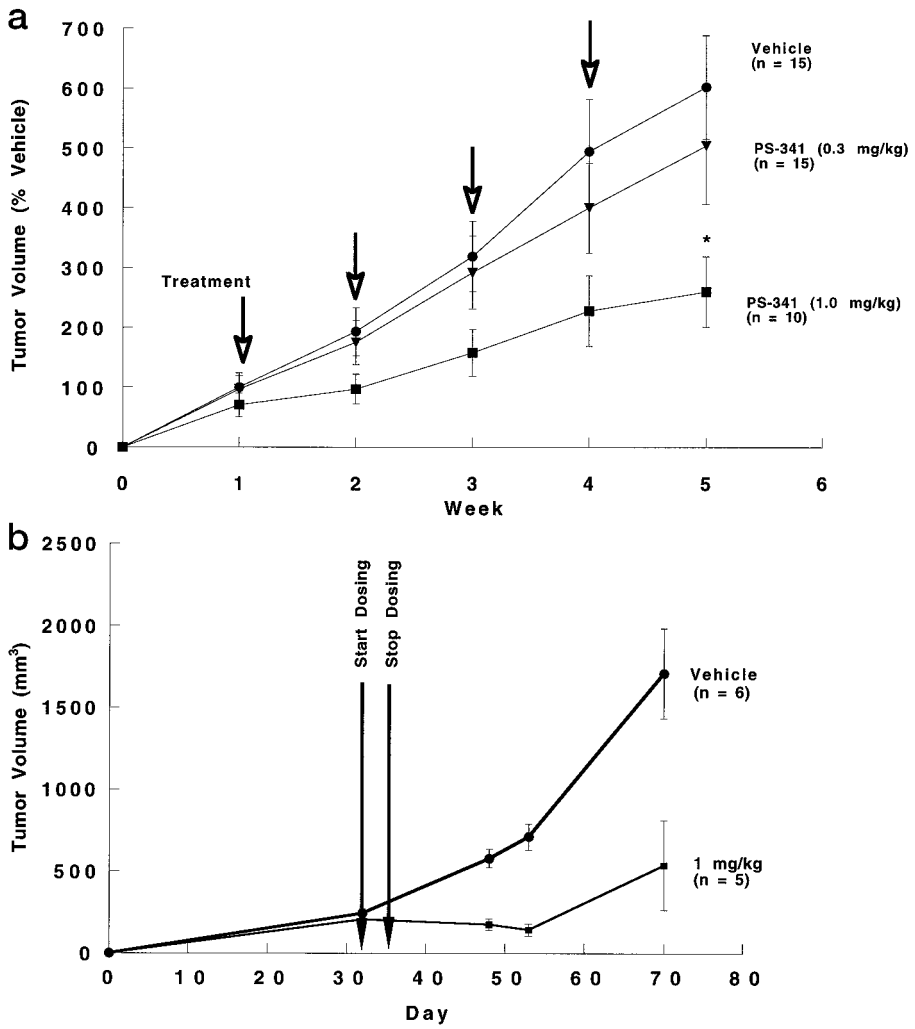

Fig. 4. Effect on PC-3 tumor growth in mice after four weekly i.v. injections of vehicle or PS-341 (*a*) or after direct injection of PS-341 or vehicle (*b*) into the PC-3 tumor on 4 consecutive days. *Data points*, tumor volumes provided as mean volumes (mm^3); *bars*, SE. *Arrows*, treatment times.

a concentration that inhibited 50% of the proteolysis (IC_{50}) of ~0.1 μM (data not shown).

In the NCI *in vitro* screen the prostate tumor PC-3 cell line (22) was shown to be sensitive to the antiproliferative effects of PS-341. To examine the potential mechanism(s) of proteasome inhibitor-induced cytotoxicity, PS-341 was studied in detail in this prostate cell line. Numerous proteins control cell cycle progression, including the tumor suppressor p53 and the CDK inhibitors p21 and p27 (12). PC-3 cells are p53 null (23), and hence, this protein is not required for PS-341-induced cytotoxicity in this cell line. In fact, PS-341 was demonstrated to be cytotoxic in multiple cell lines in the NCI screen, independent of p53 status (data not shown). Protein levels of p21 were measured to exemplify the activity of PS-341 in cells. Although very little p21 protein was detected in untreated cells, levels were significantly increased with 10 nM PS-341 (Fig. 2*A*) occurring 24 h after drug addition. The increase in p21 protein levels could be detected 4 h after PS-341 treatment (data not shown). The increase in p21 led to an inhibition in the activity but not the levels of CDK-4 after 8 h (data not shown).

The ability of PS-341 to inhibit cell cycle progression was determined by propidium iodide staining and FACS analysis. Treatment of PC-3 cells with PS-341 (100 nM) for 8 h resulted in the accumulation of cells in G_2-M, with a corresponding decrease in the number of cells in G_1 (Fig. 2*B*). A slight increase in the number of cells in S phase was also noted. These effects preceded cytotoxicity and support other data showing that increased p21 levels, in addition to blocking the G_1-S transition, also block the G_2-M transition leading to an accumulation of cells in G_2-M (24, 25). These results clearly demonstrate that PS-341 effects proteins that control cell cycle progression.

Inhibiting the degradation of key cell cycle regulatory proteins causes a disparity in the proliferative signals and can eventually lead to apoptosis. Indeed, nonselective proteasome inhibitors can arrest cell growth and activate apoptosis (26, 27). Thus, the effect of PS-341 on cell viability was evaluated. The PS-341 doses at which 50% of PC-3 cells were killed at 24 and 48 h were determined to be 100 and 20 nM, respectively (Fig. 2*C*). Moreover, nuclear condensation was noted 16–24 h after the addition of PS-341 (≥100–500 nM; data not shown). Activation of caspases occurs in cells undergoing apoptosis, and cleavage of PARP is used as an indicator of apoptosis (28). Additional studies showed that PS-341 treatment leads to PARP cleavage in a time-dependent manner (Fig. 3*A*), with concentrations as low as 100 nM being effective at 24 h (Fig. 3*B*), demonstrating that PS-341 initiates apoptosis in PC-3 cells. However, because PARP cleavage and nuclear DNA condensation were not apparent until 16 h, a time after which growth arrest was apparent, the data indicate that growth arrest precedes apoptosis and cytotoxicity.

PS-341 Inhibits PC-3 Tumor Growth in Nude Mice. The NCI examined initial activity *in vivo* with a hollow fiber assay (29), which recorded very good activity for PS-341 and a series of analogues (data not shown). This gave impetus to examine antitumor activity for PS-341 in human xenografts. For example, s.c. implantation of human PC-3 tumor cells into nude mice elicits a large tumor that is eventually

lethal. PS-341 was administered to mice injected with PC-3 cells when the tumors became palpable (>300 mm^3). Two studies were undertaken. First, mice bearing PC-3 tumors were injected with PS-341 (0.3 or 1.0 mg/kg) i.v. once weekly for 4 weeks, and tumor volumes were recorded. Weekly i.v. treatment with PS-341 (1.0 mg/kg) resulted in a significant decrease in tumor growth ~60% ($P < 0.05$), as determined by measurement of tumor volume. The lower dose of PS-341 (0.3 mg/kg) produced a 16% decrease in tumor volume but did not reach significance (Fig. 4*A*). PS-341 significantly decreased the tumor volume although distribution of the compound to the skin is limited (see below). To further explore the anticancer utility of PS-341, the drug was administered directly into PC-3 tumors in a second study. On 4 consecutive days, PS-341 (1.0 mg/kg) was administered (in 10 μl) into established PC-3 tumors, and results clearly showed a dramatic decrease in tumor burden (Fig. 4*B*). In addition to the large decrease in tumor volume (70%), two of five mice (40%) had no detectable tumors at the end of the study. At well-tolerated doses, treatment with PS-341 clearly suppressed tumor growth. These data highlight the full antitumor potential of PS-341. Similar effects have been observed in other murine tumors and human xenograft tumors (data not shown). No adverse effects of drug treatment were noted during any of these studies.

To determine the pharmacodynamics of i.v. administered PS-341, WBCs, brain, colon, liver, muscle, prostate, testes, and PC-3 tumor tissue were collected following PS-341treatment. Subsequently, residual 20S proteasome activity was determined in these samples, and results showed that PS-341 elicited a dose-dependent decrease in 20S proteasome activity. As an example, in WBCs 1.0 h after treatment, 20S proteasome activity was significantly decreased (Fig. 5*A*) and returned to baseline after 24 h. Similar effects were noted in other tissues, except the brain and testes, where no proteasome inhibition was observed, indicating that the drug did not penetrate these tissues (data not shown). Of great interest, 1.0 h after i.v. administration of PS-341, a significant decrease in 20S proteasome activity was noted in s.c. implanted PC-3 tumors, up to 40% (Fig. 5*B*). Considering that the tumor was exposed to only a fraction of the administered PS-341, the decrease in 20S proteasome activity in these tumor samples illustrates that the drug clearly has a significant effect at its target site and that such proteasome inhibition ultimately leads to decreased tumor burden, as demonstrated above.

i.v. dosing with radiolabeled [^{14}C]PS-341 to rats allowed analysis of the drug's distribution as determined by quantitative whole-body autoradiography. The highest radioactivity levels 10 min after drug administration were in the adrenals, kidney cortex, liver, prostate, and spleen. Lower levels were found throughout other organs, including the skeletal muscle, skin, and blood. The brain, spinal cord, eye, and testes had levels below the limits of quantitation. In the gastrointestinal tract, the highest radioactivity levels were found in the small intestine (Fig. 6*A*). At later time points (3 and 6 h) the same general profile was observed, although radioactivity levels in the gastrointestinal tract were the highest in the large intestine. At 24 h, the highest radioactivity levels were observed in the same organs as those seen initially but were reduced from 6 h (Fig. 6*B*). Furthermore, that no detectable levels were observed in the brain, spinal cord, eye, or testes suggest that PS-341 does not readily cross tight endothelial cell junctions. These data support the lack of 20S proteasome inhibition reported above in these organs. Because the gastrointestinal tract contained high levels of radioactivity, this distribution profile is indicative of a compound excreted via the bile. This was confirmed in rats with bile duct cannulae, where the majority (66%) of the radiolabeled drug was, indeed, excreted into the bile; the remainder was in the urine. Data from the 20S proteasome assay showed that neither

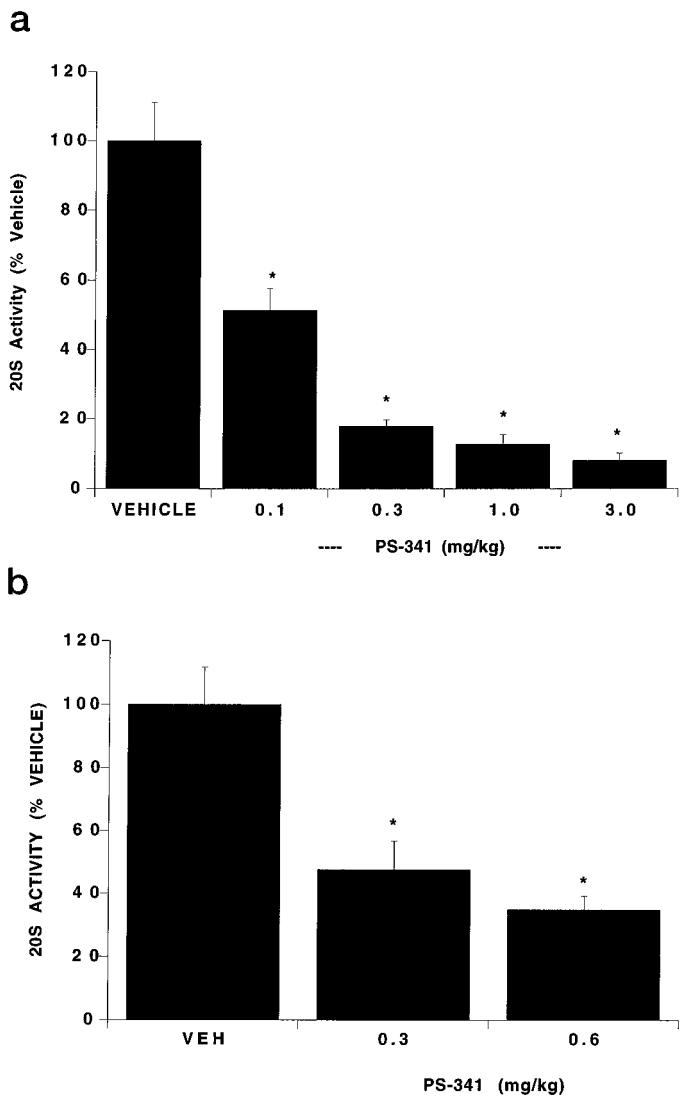

Fig. 5. Effect on 20S proteasome activity in murine WBCs (*a*) and in PC-3 tumors (*b*), 1.0 h after i.v. dosing of PS-341. *Columns*, mean percentage of control; *bars*, SE; *, statistical significance $P < 0.05$.

fluid contained inhibitory activity, suggesting that only metabolized PS-341 was excreted (data not shown).

The low levels detected in skin suggest that s.c. implanted tumor cells would have limited exposure to i.v. administered PS-341. Additional radiolabeled drug experiments in mice, bearing PC-3 tumors, also showed that i.v. PS-341 had a similar distribution to that observed in rats and that access of the drug to the skin and the tumor was limited (Fig. 7). However, only <1.0% of the injected PS-341 was detected in the tumor, but this was sufficient to significantly inhibit 20S proteasome activity in this tissue (Fig. 5*B*). Together, these studies imply that the potency of PS-341 in murine s.c. xenograft models may be underestimated. This concept appears to be confirmed because direct administration of PS-341 into the PC-3 tumor evoked complete tumor regression in 40% of the animals (Fig. 4*B*).

DISCUSSION

The fundamental goal of many chemotherapeutic agents currently used to treat neoplastic disease is to interfere with tumor cell metabolism and the mitotic process by blocking protein and DNA synthesis. This report describes a novel series of very selective inhibitors of the

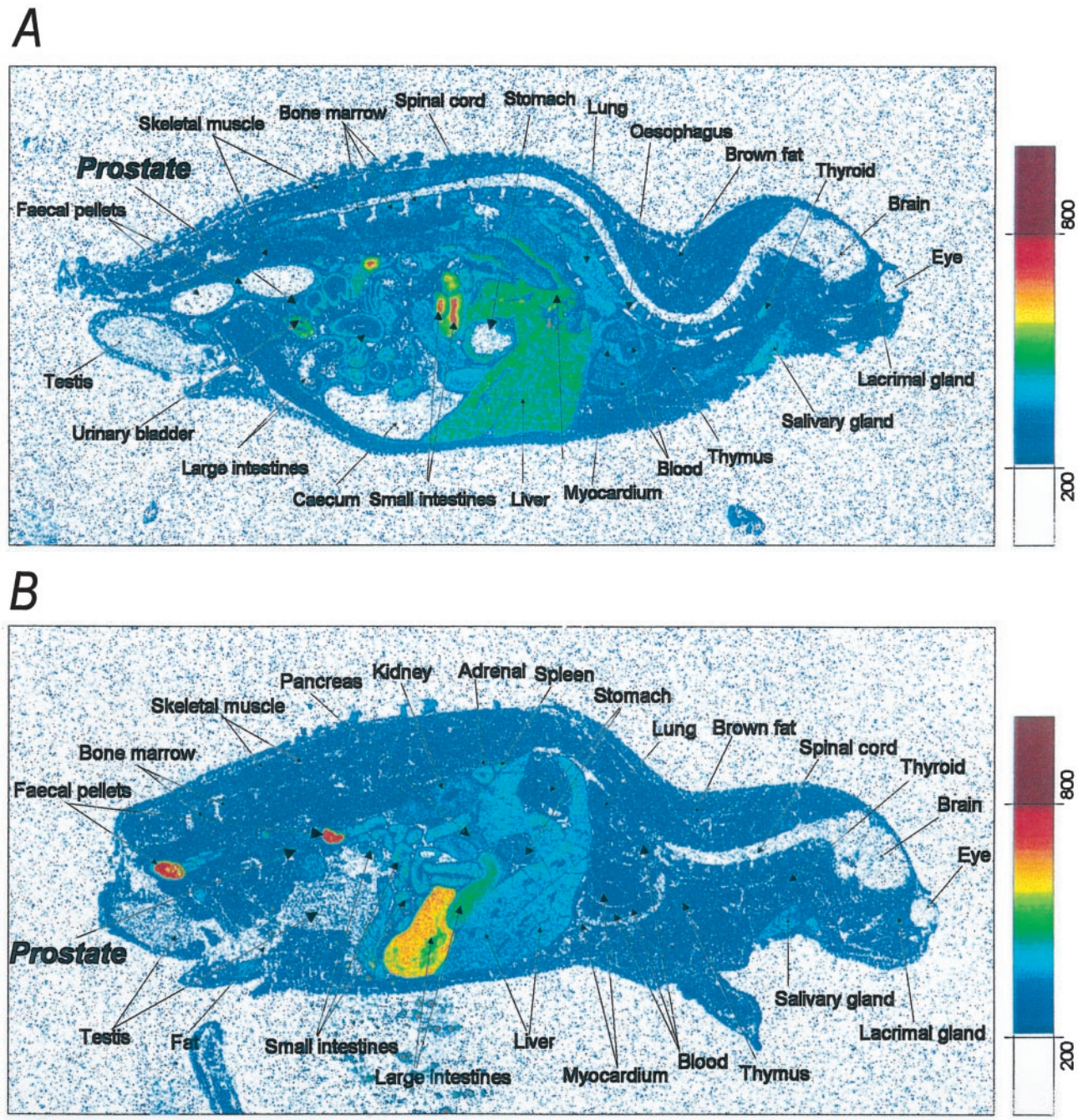

Fig. 6. Distribution of radiolabeled [^{14}C]PS-341 in rats. Sagittal sections were taken 1.0 h (*A*) and 24 h (*B*) after i.v. drug administration. *Color bar*, level of radioactivity, with *white* signifying no activity and *red* indicating the highest activity.

proteasome that serve to block cellular protein degradation. Although protein turnover is required for normal cell function, there is much data linking protein turnover to cell cycle regulation (3). As such, these data support a causal relationship between inhibition of the proteasome and inhibition of cell growth in human tumor cell lines *in vitro*. The structure-activity relationship determined here correlates very well to tumor cell growth inhibition and provided strong support that the inhibition of the biochemical target, the proteasome, was directly related to the biological effect of the compounds. Moreover, the *in vitro* data suggest that the proteasome has a significant role in maintaining cell viability and controlling cell proliferation, confirming earlier reports (30, 31).

The development of selective and potent proteasome inhibitors was based upon the above concept, with the aim of arresting uncontrolled proliferation of tumors through a multitude of mechanisms. Proteasome-induced cytotoxicity could potentially result from multiple events, including the stabilization and deregulated function of cyclins, CDK inhibitors, tumor suppressor proteins, IκB, and a large number of other proteins associated with cell cycle progression. Our report highlights the capacity of proteasome inhibitors to induce cell cycle arrest and apoptosis through inhibition of the proteasome and illustrates that these effects occur in a broad range of tumor cells.

Analysis of the inhibition data in the NCI cell line panel indicates that the proteasome inhibitors have potent and wide-ranging antitumor activity with a unique pattern of tumor inhibition, as judged by the COMPARE program (16). Further demonstration of the utility of such

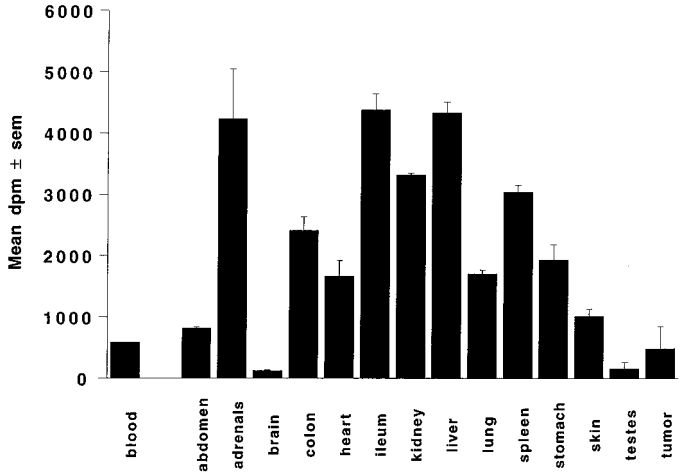

Fig. 7. Distribution of radiolabeled [^{14}C]PS-341 in various murine organs and PC-3 tumor tissue 1.0 h after i.v. drug administration. *Columns*, tissue and blood values, expressed as mean dpm/100 mg tissue (wet) weight and mean dpm/100 μl, respectively, determined using scintillation counting in homogenized samples; *bars*, SE.

compounds is evidenced by their activity in the NCI hollow fiber assays. Using the NCI screens to identify candidate agents with antitumor activity, without the prerequisite for extensive metabolism and pharmacokinetic studies, was instrumental in the rapid development of this unique class of chemotherapeutic agents. Results from mechanistic studies in the PC-3 tumor with PS-341, a representative of this new class of agents, exemplifies their activity *in vitro* to arrest cell cycle progression and cause apoptosis.

At doses that are permissive to animals, i.v. treatment of PS-341 can suppress tumor growth in many murine and human xenograft tumors. Here, we focused on the PC-3 xenograft and clearly showed the potent antitumor effects of PS-341 when it is given as a weekly i.v. treatment. PS-341 significantly ($P < 0.05$) decreased the tumor volume in these studies, although distribution of the compound to the skin is limited. The activity of PS-341 in orthotopic tumor models is currently being evaluated. However, as a proof-of-concept study, direct administration of PS-341 into the PC-3 tumor induced a dramatic decrease in tumor burden and actually produced a 40% cure rate, clearly highlighting the potential for such compounds in cancer therapy.

Due to the novel nature of proteasome inhibitors as therapeutics, it was decided to undertake a full toxicological evaluation of PS-341, not only in rodents but in the highest species possible, primates. On the basis of these studies, maximum tolerated doses and side effect profiles of PS-341 were established. The main adverse effect noted in both species was gastrointestinal toxicity as anticipated from the distribution studies. In primates, this was seen as a decrease in food intake (anorexia), emesis, and diarrhea, which all occurred in a dose-related manner. No other signs of toxicity were noted in these studies, although full clinical chemistry, hematology, and microscopic analysis of over 40 tissues were examined. Modest effects of PS-341 were seen in the spleen and the thymus, where lymphocytic depletion was reported. These findings are not unexpected because there are reports in the literature with other proteasome inhibitors showing that they regulate T-cell proliferation (32). Of interest, PS-341 did not induce bone marrow toxicity, suggesting that it either does not affect hematopoetic cells here or that it has limited access to such cells.

The *ex vivo* 20S proteasome assay will be invaluable not only to follow the pharmacodynamics of PS-341 but also to help in early clinical trials to evaluate its effectiveness at its biochemical target, the proteasome, and its intended site, the tumor. The assay may also be used to correlate proteasome activity with toxicity to help determine dose escalation in clinical trials.

Although several reports document the cytotoxic effects of other less potent and nonselective proteasome inhibitors (26, 27, 30, 31), our findings represent the first attempt to systematically correlate proteasome inhibition potency with tumor cell killing using a novel, selective family of inhibitors. Furthermore, we demonstrate that such agents are broadly active against multiple tumor cell types *in vitro* and *in vivo*. The full impact of the antitumor activity of PS-341 will be determined upon completion of the clinical trials.

ACKNOWLEDGMENTS

We thank Dr. Craig Hilton for his help with the FACS analysis and Dr. Al Baldwin for his constructive comments on the manuscript.

REFERENCES

1. Goldberg, A. L., Stein, R., and Adams, J. New insights into proteasome function: from Archaebacteria to drug development. Chem. Biol., *2:* 503–508, 1995.
2. Coux, O., Tanaka, K., and Goldberg, A. L. Structure and function of the 20S and 26S proteasomes. Annu. Rev. Biochem., *65:* 801–847, 1996.
3. King, R. W., Deshaies, R. J., Peters, J-M., and Kirschner, M. W. How proteolysis drives the cell cycle. Science (Washington DC), *274:* 1652–1659, 1996.
4. Chau, V., Tobias, J. W., Bachmair, A., Marriott, D., Ecker, D. J., Gonda, D. K., and Varshavsky, A. A multiubiquitin chain is confined to specific lysine in a targeted short-lived protein. Science (Washington DC), *243:* 1576–1583, 1989.
5. Palombella, V. J., Rando, O. J., Goldberg, A. L., and Maniatis, T. The ubiquitin-proteasome pathway is required for processing the NF-κB1 precursor protein and the activation of NF-κB. Cell, *78:* 773–785, 1994.
6. Beg, A. A., and Baltimore, D. An essential role for NF-κB in preventing TNF-α-induced cell death. Science (Washington DC), *274:* 782–784, 1996.
7. Van Antwerp, D. J., Martin, S. J., Kafri, T., Green, D. R., and Verma, I. M. Suppression of TNF-α-induced apoptosis by NF-κB. Science (Washington DC), *274:* 787–789, 1996.
8. Wang, C-Y., Mayo, M. W., and Baldwin, A. S. TNF- and cancer therapy-induced apoptosis: potentiation by inhibition of NF-κB. Science (Washington DC), *274:* 784–787, 1996.
9. Chu, Z-L., McKinsey, T. A., Liu, L., Gentry, J. J., Malim, M. H., and Ballard, D. W. Suppression of tumor necrosis factor-induced cell death by inhibitor of apoptosis c-IAP2 is under NF-κB control. Proc. Natl. Acad. Sci. USA, *94:* 10057–10062, 1997.
10. Zetter, B. R. Adhesion molecules in tumor metastasis. Semin. Cancer Biol., *4:* 219–229, 1993.
11. Read, M. A., Neish, A. S., Luscinskas, F. W., Palombella, V. J., Maniatis, T., and Collins, T. The proteasome pathway is required for cytokine-induced endothelial-leukocyte adhesion molecule expression. Immunity, *2:* 493–506, 1995.
12. Sherr, C. J. Cancer cell cycles. Science (Washington DC), *274:* 1672–1677, 1996.
13. Adams, J., Behnke, M., Chen, S., Cruickshank, A. A., Dick, L. R., Grenier, L., Klunder, J. M., Ma, Y-T., Plamondon, L., and Stein, R. L. Potent and selective inhibitors of the proteasome: dipeptidyl boronic acids. Bioorg. Med. Chem. Lett., *8:* 333–338, 1998.
14. Stein, R. L., Melandri, F., and Dick, L. Inhibition of the chymotryptic-like proteolytic activity of rabbit muscle 20S proteasome. Proteasome isolation, purification, and assays were performed as previously described. Biochemistry, *35:* 3899–3908, 1996.
15. Boyd, M. R., and Paull, D. Some practical considerations and applications of the National Cancer Institute *in vitro* anticancer drug discovery screen. Drug Dev. Res., *34:* 91–109, 1995.
16. Weinstein, J. N., Myers, T. G., O'Connor, P. M., Friend, S. H., Fornace, A. J., Kohn, K. W., Fojo, T., Bates, S. E., Rubinstein, L. V., Anderson, N. L., Buolamwini, J. K., van Osdol, W. W., Monks, A. P., Scudiero, D. A., Viswanadhan, V. N., Johnson, G. S., Wittes, R. E., and Paull, K. D. An information-intensive approach to the molecular pharmacology of cancer. Science (Washington DC), *275:* 343–349, 1997.
17. Mosmann, T. Rapid colorimetric assay for cellular growth and survival: application to proliferation and cytotoxicity assays. J. Immunol. Methods, *65:* 55–63, 1983.
18. Noguchi, P. D. Use of flow cytometry for DNA analysis. Curr. Protocol Immunol., *57:* 1–8, 1996.
19. Tsubuki, S., Kawasaki, H., Saito, Y., Miyashita, N., Inomata, M., and Kawashima, S. Purification and characterization of a Z-Leu-Leu-MCA degrading protease expected to regulate neurite formation: a novel catalytic activity in proteasome. Biochem. Biophys. Res., *196:* 1195–1201, 1993.
20. Adams, J., and Stein, R. Novel inhibitors of the proteasome and their therapeutic use in inflammation. Annu. Rep. Med. Chem., *31:* 279–288, 1996.
21. Seemüller, E., Lupas, A., Stock, D., Löwe, J., Huber, R., and Baumeister, W. Proteasome from *Thermoplasma acidophilum*: a threonine protease. Science (Washington DC), *268:* 579–582, 1995.
22. Kaighn, M. E., Narauam, K. S., Ohnuki, Y., Lechner, J. F., and Jones, L. W. Establishment and characterization of a human prostatic carcinoma cell line (PC-3). Invest. Urol., *17:* 16–23, 1979.

23. Tang, D. G., Li, L., Chopra, D. P., and Porter, A. T. Extended survivability of prostate cancer cells in the absence of trophic factors: increased proliferation, evasion of apoptosis, and the role of apoptosis proteins. Cancer Res., *58:* 3466–3479, 1998.
24. Machiels, B. M., Henfling, M. E. R., Gerards, W. L. H., Broers, J. L. V., Bloemendal, H., Ramaekers, F. C. S., and Schutte, B. Detailed analysis of cell cycle kinetics upon proteasome inhibition. Cytometry, *28:* 243–252, 1997.
25. Dulic, V., Stein, G. H., Far, D. F., and Reed, S. I. Nuclear accumulation of p21Cip1 at the onset of mitosis: a role at the G_2/M-phase transition. Mol. Cell. Biol., *18:* 546–557, 1998.
26. Drexler, H. C. A. Activation of the cell death program by inhibition of proteasome function. Proc. Natl. Acad. Sci. USA, *94:* 855–860, 1997.
27. Orlowski, R. Z., Eswara, J. R., Lafond-Walker, A., Grever, M. R., Orlowski, M., and Dang, C. V. Tumor growth inhibition induced in a murine model of human Burkitt's lymphoma by a proteasome inhibitor. Cancer Res., *58:* 4342–4348, 1998.
28. Nicholson, D. W., Ali, A., Thornberry, N. A., Vaillancourt, J. P., Ding, C. K., Gallant, M., Gareau, Y., Griffin, P. R., Labelle, M., Lazebnik, Y. A., Munday, N. A., Raju, S. M., Smulson, M. E., Yamin, T. T., Yu, V. L., and Miller, D. K. Identification and inhibition of the ICE/CED-3 protease necessary for mammalian apoptosis. Nature (Lond.), *37:* 37–43, 1995.
29. Hollingshead, M. G., Alley, M. C., Camalier, R. F., Abbott, B. J., Mayo, J. G., Malspeis, L., and Grever, M. R. *In vivo* cultivation of tumor cells in hollow fibers. Life Sci., *57:* 131–141, 1995.
30. Imajoh-Ohmi, S., Kawaguchi, T., Sugiyama, S., Tanaka, T., Omura, K., and Kikuchi, H. Lactacystin, a specific inhibitor of the proteasome, induces apoptosis in human monoblast U937 cells. Biochem. Biophys. Res. Commun., *217:* 1070–1077, 1995.
31. Lopes, U. G., Erhardt, P., Yao, R., and Cooper, G. M. p53-dependent induction of apoptosis by proteasome inhibitors. J. Biol. Chem., *272:* 12893–12896, 1997.
32. Wang, X., Luo, H., Chen, H., Duguid, W., and Wu, J. Role of proteasomes in T cell activation and proliferation. J. Immunol., *160:* 788–801, 1998.